IEEE Access
Multidisciplinary | Rapid Review | Open Access Journal

Received September 21, 2020, accepted October 25, 2020, date of publication October 29, 2020,
date of current version November 12, 2020.

Digital Object Identifier 10.1109/ACCESS.2020.3034599

Parallel PPDU Transmission Mechanism for Wideband Wireless LANs

SHINNAZAR SEYTNAZAROV[1], DONG GEUN JEONG[2,3], (Senior Member, IEEE), AND WHA SOOK JEON[1], (Senior Member, IEEE)

[1]Department of Computer Science and Engineering, Seoul National University, Seoul 08826, South Korea
[2]Department of Electronics Engineering, Hankuk University of Foreign Studies, Yongin 17035, South Korea
[3]Applied Communication Research Center, Hankuk University of Foreign Studies, Yongin 17035, South Korea

Corresponding author: Wha Sook Jeon (wsjeon@snu.ac.kr)

This work was supported in part by the National Research Foundation of Korea (NRF) Grant funded by the Ministry of Science and Information and communication Technologies (MSIT) of Korean Government under Grant NRF-2019R1F1A1062597.

ABSTRACT When the preambles of a wideband 802.11n/ac frame transmission are affected by a collision with a 20MHz frame on one of the subchannels, a receiver might fail to decode the whole wideband frame. Experimental evaluations with off-the-shelf 802.11n hardware showed that the vulnerability of wideband frame transmission to a narrowband collision/interference is a real problem. To mitigate the severe impact of narrowband collision/interference on wideband transmission, we propose to transmit several 20MHz frames in parallel instead of a single wideband frame so that a narrowband collision on one of the subchannels affects only the parallel frame transmitted on that subchannel. Performance evaluations demonstrated that the proposed parallel frame transmission scheme significantly improves the throughput and delay performance of wideband transmissions under different traffic and channel conditions. While the throughput performance of the proposed scheme for saturated traffic conditions was analytically validated, extensive simulation-based evaluations showed that the proposed scheme achieves great performance improvement for unsaturated traffic conditions and hidden node environment.

INDEX TERMS 802.11, wireless local area network (WLAN), channel bonding, wide channel access, parallel transmission, narrowband collision.

I. INTRODUCTION

In recent years, wireless local area network (WLAN) technology has achieved tremendous improvements in both physical (PHY) and medium access control (MAC) layers. One of such improvements is the capability to use much wider channels than traditional 20MHz-wide channels. Initially, the IEEE 802.11n high throughput (HT) standard introduced the use of a 20MHz-wide primary channel (PCH) together with another 20MHz-wide secondary channel (SCH) to transmit 40MHz PHY layer conformance procedure (PLCP) protocol data units (PPDUs), i.e., 40MHz frames [1]. Later, the IEEE 802.11ac very high throughput (VHT) standard introduced the use of much wider 80 and 160MHz-wide channels [2].

Since the main goal of the wideband transmission is to enhance the throughput and capacity performance of WLAN, most of the existing research works related to wideband transmission aim to find effective ways to distribute available channels among WLANs and analyze the performance of wide channel access with different methods under different conditions [3]–[8]. However, according to the wideband HT/VHT PHY packet structure explained in the following paragraph, the wideband transmission can be much more vulnerable to narrowband interference, which may be a big obstacle to fulfill the expected performance improvement.

Figure 1 depicts 40MHz HT (802.11n) and 80MHz VHT (802.11ac) PHY packet structures. Wideband transmissions start with legacy preambles duplicated over all 20MHz subchannels and followed by HT/VHT preamble, Service field, HT/VHT data, MAC and PHY padding, and Tail fields. The legacy preambles are all in a 20MHz-form and used for transmission detection, time synchronization, and channel estimation for each of the 20MHz subchannels. The HT/VHT preambles inform the receiver about the transmission settings and are also used for multiple-input/multiple-output (MIMO) channel estimation and pilot subcarrier tracking purposes. The Service field is in a wideband form and used to initialize the descrambler of the receiver [1], [2]. Although

The associate editor coordinating the review of this manuscript and approving it for publication was Arun Prakash.

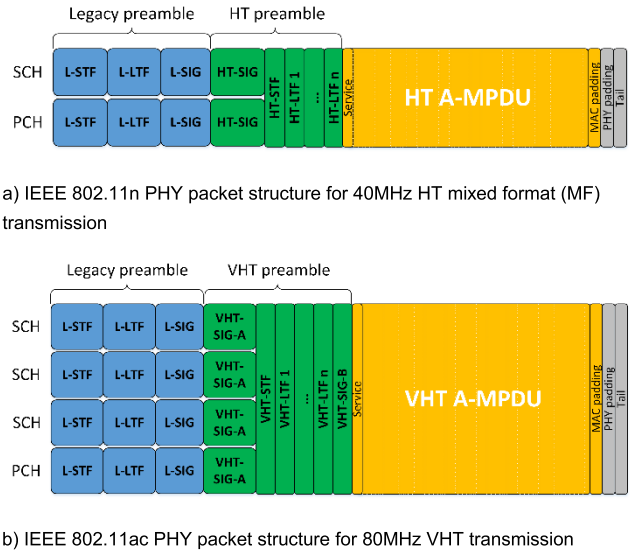

FIGURE 1. **PHY packet structure for wideband transmissions.**

simultaneously using n 20MHz-wide subchannels increases the transmission rate of wideband PPDU payload by about n times, however, if PHY preambles of wideband PPDU are affected by a narrowband collision on any of the subchannels, such a narrowband collision adversely affects synchronization, MIMO channel estimation, and descrambler initialization, and consequently may lead to the decoding error of a whole wideband PPDU.

On the other hand, it is well known that the link rate adaptation technique, which adjusts the PHY transmission rate according to link quality, is effective to cope with interference. However, in the IEEE 802.11n/ac, the link adaption is applied for the entire wideband channel, not separately for each 20MHz subchannel. That is, the narrowband interference on a subchannel can result in the low PHY rate of wideband transmission, or incur a narrowband collision mentioned above. Accordingly, the problem of narrowband interference in wideband WLANs needs to be dealt with more importance to avoid severe performance degradation.

To combat the hidden interference on SCHs, a mechanism to negotiate available bandwidth information between the sender and receiver through enhanced request-to-send (RTS)/clear-to-send (CTS) was introduced in [9] and became a part of the IEEE 802.11ac standard [2]. While the enhanced RTS/CTS achieves performance gains in the presence of hidden interference on SCHs, the mechanism also introduces an undesirable overhead which is sometimes larger than the transmission duration of actual data PPDU. To alleviate such undesirable overhead caused by RTS/CTS exchange, a new scheme that adaptively turns on/off RTS/CTS based on inferred knowledge about the presence/absence of hidden interference was proposed in [10]. Besides, Byeon *et al.* studied an adverse impact of time-domain interference, which does not overlap with the desired signal in the frequency domain, and proposed an operating channel bandwidth adaptation algorithm which mitigates the impact of such interference [11].

While the existing works in literature mainly try to solve serious performance degradation problems related to interference and channel allocation, the fundamental problem related to the vulnerability of existing wideband PHY packet structure to collision/interference on one of the subchannels stays untouched. This article has the following major contributions. First, we show the vulnerability of the existing wideband PHY structure to narrowband collision/interference by the means of real experiments. Second, we propose a new parallel PPDU transmission scheme, which mitigates the severe impact of narrowband collision/interference on throughput and delay performance by transmitting several 20MHz-wide PPDUs in parallel. Third, we analytically validate the throughput performance of the proposed scheme under the saturated traffic condition. Last but not the least, using simulations we show that the proposed scheme achieves great throughput and delay improvements under unsaturated traffic conditions and in the presence of hidden nodes.

The remaining parts of this work are organized as follows. As background, Section II discusses distributed coordination function (DCF) protocol, frame aggregation, wide channel access mechanisms in 802.11n/ac, existing wideband PHY packet structures, its vulnerability to narrowband interference, and other related works in literature. Section III presents a newly proposed parallel PPDU transmission mechanism for wideband WLANs and its throughput performance model in comparison with baseline 802.11ac wideband transmission. Section IV discusses performance evaluation. Finally, Section V concludes this work.

II. BACKGROUND

A. DCF PROTOCOL AND A-MPDU AGGREGATION

The IEEE 802.11 technologies use the DCF protocol for data transfer. A station that has a packet to transmit continuously monitors the channel. If the channel is sensed idle for a period called DCF inter-frame space (DIFS), the station randomly chooses a new backoff counter b from $[0, W-1]$ range, and decrements the b at the end of each idle backoff slot (σ), where W is the minimum contention window size. If the station senses the channel busy while $b > 0$, it freezes the b to its current value and resumes decrement only after an idle DIFS period. Once the backoff counter expires, i.e., b becomes zero, the station transmits its PPDU. If the receiver successfully receives the PPDU, it replies with an acknowledgment (ACK) frame. If the sender does not receive ACK within a timeout, it randomly chooses a new backoff counter from $[0, W_1 - 1]$ range after an idle DIFS period where $W_i = 2^i \cdot W$ is the contention window size at the backoff stage i. If the sender receives ACK within timeout, it resets the backoff stage to 0 and initiates another backoff process after an idle DIFS if it has a packet to send. If the PPDU transmission fails at stage m, the PPDU is discarded and the backoff stage is reset [1], [12].

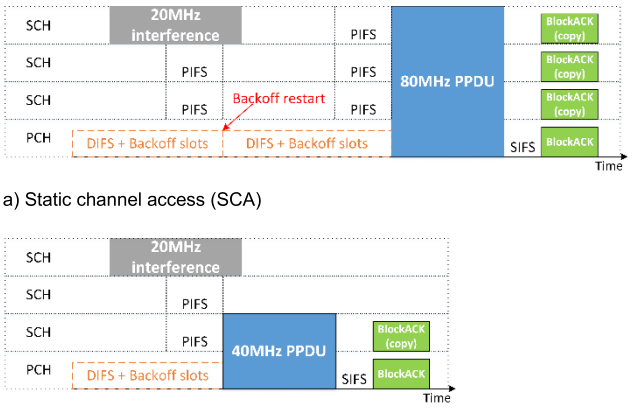

FIGURE 2. Wide channel access in IEEE 802.11ac.

The IEEE 802.11n standard introduced the aggregate MAC protocol data unit (A-MPDU) aggregation scheme, which allows the sender station to transmit up to 64 MAC protocol data units (MPDUs) upon single channel access. If the intended receiver receives at least one of the MPDUs successfully, it replies with a block acknowledgment (BlockACK) frame indicating which MPDUs were successful, so the sender will retransmit only the unsuccessful MPDUs upon the next channel access [1], [12].

B. WIDE CHANNEL ACCESS IN BASELINE IEEE 802.11n/ac WLANs

Traditionally, legacy IEEE 802.11 WLANs used 20MHz-wide channels. However, the IEEE 802.11n introduced an optional 40MHz channel: a 40MHz-capable sender can use 20MHz PCH together with the next 20MHz-wide orthogonal channel called SCH as if they become a single 40MHz channel [1]. Later, the IEEE 802.11ac standard introduced mandatory 80MHz and optional 160MHz channels [2]. The standard specifies two mechanisms for wide channel access: static channel access (SCA) and dynamic channel access (DCA) [1], [2]. In SCA, a sender transmits only when all SCHs are available for transmission. More specifically, the station performs a DCF-based random backoff procedure on PCH. When its backoff timer expires, the station checks whether SCHs have been idle for a period called point coordination function inter-frame space (PIFS). If the station finds all SCHs idle during the last PIFS, it transmits a wideband PPDU over PCH and all SCHs; otherwise, it restarts the backoff procedure with the same contention window size. Figure 2a illustrates a case where the 802.11ac sender wants to send an 80MHz PPDU. During PIFS before the backoff expiration, the sender finds the third SCH occupied by another transmission, thus it restarts the backoff procedure with the same contention window size. Upon the next backoff expiration, the sender senses all subchannels idle and thus transmits an 80MHz PPDU. In response, the receiver sends back 20MHz BlockACK frames replicated over every subchannel used by the sender [12].

Contrary, in DCA, upon the backoff timer expiration, the station uses only idle SCHs to make a valid 20, 40, or 80MHz channel [1], [2]. Figure 2b illustrates the same case as in Figure 2a but with a DCA-capable sender. When the sender senses the third SCH busy during PIFS before backoff expiration, it decreases the transmit channel bandwidth to the next narrower valid bandwidth, i.e., 40MHz bandwidth, which includes the PCH and the first SCH. If any of the packets from the 40MHz PPDU was successfully received, the receiver replies with 20MHz BlockACK frames replicated over each subchannel used by the sender [12].

C. PHY PACKET STRUCTURE OF EXISTING WIDEBAND WLANS

Figure 1 depicts the PHY packet structures of 40MHz HT (802.11n) and 80MHz VHT (802.11ac) transmissions. For the coexistence purpose with 20MHz stations, the wideband PHY packet structure begins with a legacy 802.11a-style preamble replicated over each 20MHz channel of wideband transmission. The legacy preamble has three fields and they have the following responsibilities [1], [2], [12]:

- The legacy short training field (L-STF) is used by the listening stations for start-of-packet detection, automatic gain control (AGC), initial frequency offset estimation, and initial time synchronization.
- The legacy long training field (L-LTF) is used for better frequency-offset estimation, synchronization, and most importantly channel estimation, which allows for correctly decoding orthogonal frequency division multiplexing (OFDM) symbols of L-SIG and VHT-SIG-A.
- The legacy signal (L-SIG) field includes the PHY transmission rate and length information. By using this field, the listening stations can estimate the duration of the remaining part of this transmission, thus they can know how long they shall not try to access the medium. When the L-SIG is a part of 802.11n/ac transmission, the Rate subfield is always set to 6.0 Mbps (the lowest 802.11a rate) and the Length subfield is set in a way that the estimated transmission duration gives the actual remaining duration of 802.11n/ac transmission.

After the legacy preamble, the HT/VHT preamble starts, which includes the HT/VHT signal, STF, and LTF fields.

- HT signal (HT-SIG) is in 20MHz-form and replicated over PCH and SCH. HT-SIG includes two OFDM symbols, HT-SIG$_1$ and HT-SIG$_2$. HT-SIG$_1$ informs the HT-capable receiver station about total bandwidth (BW) of current PPDU, modulation and coding scheme (MCS) level used for PPDU payload transmission, and length of

The 802.11n standard introduced two transmission formats. First, a mandatory HT mixed format (MF) which includes legacy preamble and thus can be detected by legacy stations as valid 802.11 transmission. Second, an optional HT greenfield format (GF) which does not include legacy preamble. In this work, we consider only HT MF format and simply call it HT throughout the paper.

the PPDU payload. HT-SIG$_2$ field informs the receiver about the type of guard interval (GI), the number of spatial streams (NSS), and cyclic redundancy check (CRC) of the HT-SIG field.

- VHT signal-A (VHT-SIG-A) field is in a 20MHz-form and is duplicated over each 20MHz channel of a wideband VHT PPDU. It includes information on BW, GI, MIMO settings, beamforming, MCS level, and other VHT-specific parameters that are used by the receiving VHT-capable stations to correctly decode the remaining wideband part of the transmission.
- HT and VHT STFs are in a wideband waveform and are used to improve the AGC setting for MIMO transmission.
- HT and VHT LTFs are in a wideband waveform and are used for MIMO channel estimation and pilot subcarrier tracking purposes. The number of LTF symbols depends on the number of spatial streams used in MIMO transmission.
- VHT-SIG-B is in a wideband waveform and is used to set up the data rate and MIMO tuning for multi-user (MU) transmission.

HT/VHT preambles are followed by the Service field which includes scrambler initialization bits that are used to synchronize the descrambler of the receiving station, HT/VHT A-MPDU, MAC and PHY padding (if necessary), and Tail fields.

D. VULNERABILITY OF WIDEBAND PPDU TO A NARROWBAND COLLISION

Wideband IEEE 802.11n/ac PPDUs are vulnerable to a collision with narrower PPDU. We can differentiate two kinds of collision:

- In the first collision type, the PHY preambles of wideband PPDU (i.e., the legacy and HT/VHT preambles) are affected by a collision with the narrowband transmission. Depending on signal and interference levels, such a collision can eventually result in decoding errors of a whole wideband PPDU at the receiver side.
- On the other hand, in the presence of hidden nodes, usually, there is another kind of collision where a narrowband transmission collides with an ongoing wideband PPDU transmission which was already synchronized by the receiver, i.e., the receiver already successfully decoded the legacy and HT/VHT preambles of the wideband PPDU and currently receiving the HT/VHT A-MPDU bits. In such a case, depending on the signal and interference levels, the receiver might fail to correctly decode the MPDUs of the wideband A-MPDU that are affected by this narrowband collision.

To demonstrate the impact of the narrowband collision on the performance of the wideband transmission, we conducted the following simple experiment. There are 802.11n and 802.11a (11n and 11a, shortly) sender and receiver pairs as shown in Figure 3. The 11n and 11a senders are hidden

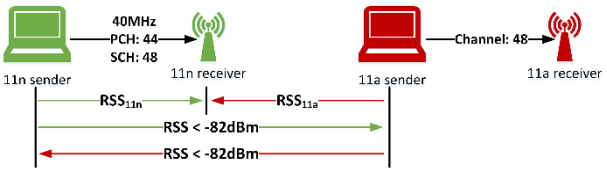

FIGURE 3. Experiment topology.

from each other since their received signal strengths (RSSs) are less than the signal detection RSS threshold value of −82dBm [1], [2], [12]. The buffers of both senders are always saturated with best-effort (BE) packets of user datagram protocol (UDP) with 1000 bytes payload. The 11n sender transmits A-MPDUs (of up to 32 packets) using long GI (LGI), MCS 7, and 40MHz channel bandwidth, where the channels 44 and 48 are used as PCH and SCH, respectively. The 11a sender transmits on channel 48 at a PHY transmission rate of 54Mbps. Since the 11a sender uses the SCH of 11n, it may generate an undesirable narrowband collision/interference at the 11n receiver. The following hardware and software were used in our experiments. The senders are laptops running Ubuntu operating system and equipped with 802.11abgn capable Atheros AR9832 wireless chipsets that are supported by ath9k driver [13]. The receivers are 802.11abgn capable TL-WDR4300 access points that support OpenWRT. UDP traffic is generated using iPerf [14].

Figure 4 depicts the average 11n throughput, access delay, and aggregation size performance for different RSS values of the target and interference signals sensed at the 11n receiver. More specifically, the performance of wideband 11n transmissions with RSS (RSS_{11n}) of −50dBm and −60dBm at 11n receiver was recorded in the presence of no interference, the narrowband interference with RSS (RSS_{11a}) of −73dBm, and −64dBm by the 11a sender on the SCH.

First, let us examine the case when the 11a sender is not active, i.e., no interference is present on the SCH of the 11n receiver. Although we say there is no interference when the 11a sender is inactive, however, there is always a very small interference from the neighboring stations which sometimes causes MPDU transmission errors in wideband A-MPDU. As one can expect, the higher the RSS_{11n}, the less the transmission errors, and thus the throughput is higher as shown in *no interference* column of Figure 4a. More specifically, the average 11n throughput is about 106.5Mbps at the RSS_{11n} of −50dBm and 88Mbps when the RSS_{11n} is −60dBm. The average access delays are about 110μs at the RSS_{11n} of −50dBm and 150μs at the RSS_{11n} of −60dBm which correspond to the sum of arbitrary IFS (AIFS) and average backoff slots at the initial backoff stage of the BE access category plus delays in hardware operations such as A-MPDU construction, BlockACK reception, and processing. In other words, wideband A-MPDUs are delivered at their

The access delay of a frame is an elapsed time between the instants of time when this frame becomes head-of-line and its successful transmission starts.

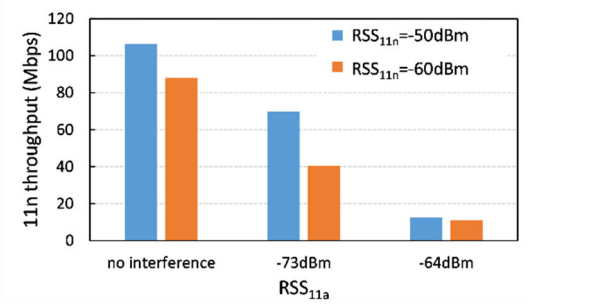

a) Average 11n throughput

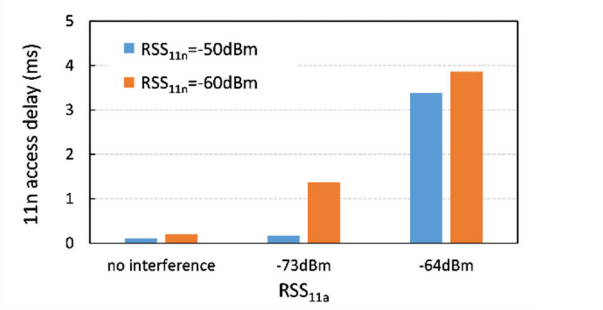

b) Average 11n access delay

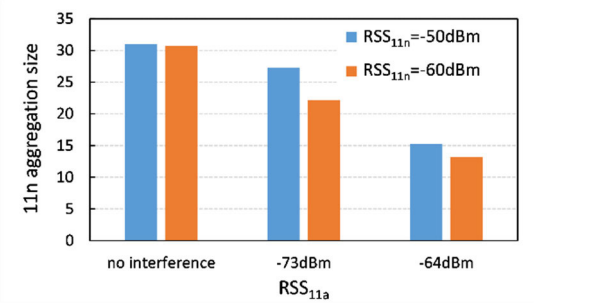

c) Average 11n aggregation size

FIGURE 4. 11n throughput and access delay performance for different signal and interference levels.

first transmission attempt. The average aggregation sizes are about 31.0 at the RSS_{11n} of −50dBm and 30.7 at the RSS_{11n} of −60dBm; they are slightly smaller than 32 which is the maximum aggregation size limit in ath9k driver. As previously mentioned there is always a small background interference which sometimes results in MPDU transmission errors and thus retransmissions. In the presence of retry MPDUs in transmit buffers, a standard automatic repeat-request (ARQ) error-control protocol called a sliding BlockACK window (BAW) mechanism, which has a window size of 64, is responsible for in-sequence delivery of the MPDUs to the upper layer of the receiver and thus, does not allow the transmission of MPDUs whose sequence numbers (SNs) are not in the range of current window [1], [2], [12]. When MPDU errors exist, the operation of the sliding BAW mechanism results in an overall decreased average aggregation size; the more the transmission errors, the smaller the average aggregation size becomes. Thus, a small number of errors caused by the interference in the background result in the average aggregation sizes that are slightly smaller than 32 [15].

Next, we examine the performance degradation of wideband transmissions in the presence of narrowband interference. The 11a sender starts transmitting saturated traffic to the 11a receiver. Since the 11n and 11a senders cannot sense the transmission of each other, they concurrently transmit instead of sharing the medium. Thus, a wideband target signal often collides with narrowband interference on the SCH of the 11n receiver. In general, the average throughput decreases as the target signal to interference ratio (SIR) decreases as depicted in Figure 4a.

As mentioned earlier in this subsection, there are two types of collisions between wideband and narrowband signals. In the first case, the PHY preambles of wideband PPDU are affected by the narrowband interference on channel 48. Since PHY preambles are used by the receiver for AGC setting, frequency offset estimation, synchronization, channel estimation, etc, the 11n receiver might fail to decode the whole wideband PPDU if those preambles are not correctly received. The possibility of such PPDU decoding failure increases as SIR decreases. The decoding failure of wideband PPDU causes its retransmission and consequently increases its access delay. Thus, this type of collision can be characterized in terms of average access delay performance depicted in Figure 4b. As interference (RSS_{11a}) increases or signal level (RSS_{11n}) decreases, i.e., as the SIR deteriorates, the average 11n access delay increases. More specifically, when RSS_{11a} is −73dBm, the average 11n access delay is about 0.17ms and 1.37ms at the RSS_{11n} of −50dBm and −60dBm, respectively. When interference strength increased to RSS_{11a} of −64dBm, the average access delay increases to 3.4ms and 3.9ms at the RSS_{11n} of −50dBm and −60dBm, respectively.

The second type of collision occurs when the narrowband 11a transmission collides with the ongoing wideband transmission which was already synchronized by the 11n receiver (i.e., PHY preambles were already successfully received) and the receiver is currently decoding the wideband A-MPDU bits. Since this kind of collision affects only the payload of the wideband PPDU, the affected MPDUs by this collision are either correctly received or un-decodable depending on the SIR levels. In the presence of transmission errors, the BAW mechanism solely determines the aggregation size since the buffers are always saturated as explained earlier. Thus, this type of collision can be mainly characterized by average aggregation size performance depicted in Figure 4c. As SIR deteriorates, the average 11n aggregation size significantly decreases. More precisely, when RSS_{11a} is −73dBm, each 11n PPDU carries about 27 and 22 packets on average at RSS_{11n} of −50dBm and −60dBm, respectively. When interference strength increases to RSS_{11a} of −64dBm, the average

Refer to [15] for more information about BAW mechanism and its impact on the aggregation size under erroneous channel conditions.

aggregation size is about 15 and 13 at RSS_{11n} of −50dBm and −60dBm, respectively.

In summary, the experimental results demonstrate that the wideband transmission performance can be severely degraded by the narrowband interference from a neighboring station.

E. WIDE CHANNEL ACCESS USING VHT RTS/CTS

In [9], Gong *et al.* proposed an enhanced version of the traditional RTS/CTS channel reservation mechanism to avoid hidden interference on the SCH; later the proposal was adopted in the 802.11ac standard [2]. A sender sends an enhanced RTS frame replicated over all 20MHz subchannels that it intends to use. The RTS frame contains two additional information: i) the total bandwidth the sender wants to use, and ii) whether the sender supports the DCA or only the SCA. The receiver continuously monitors all subchannels using a clear channel assessment (CCA). If the receiver senses one of the subchannels busy during PIFS before the RTS reception starts, it acts in one of the following ways:

- If the sender or receiver does not support the DCA, the receiver does not respond with a CTS, implicitly signaling the sender about the unavailability of requested channel bandwidth at the receiver. The sender restarts the CSMA/CA backoff with the same contention window size.
- If both of the stations support the DCA, then the receiver replies with a 20MHz CTS frame duplicated on all available subchannels that make up a valid wideband channel. The sender then transmits a data PPDU over available subchannels.

If all subchannels are sensed idle during PIFS before the RTS reception starts, the receiver replies with the CTSs duplicated over all subchannels and thus the sender sends wideband data PPDU utilizing all subchannels.

F. OTHER RELATED WORKS IN LITERATURE

There are many works related to wideband channel operations in 802.11 networks. Here we talk briefly about some of them. The authors in [3] and [4], proposed an analytical framework to model the performance of wide channel access for multiple WLANs coexisting together under a saturated traffic scenario. The authors of [5] and [6] analytically studied the performance of a wideband WLAN coexisting with a legacy WLAN operating on the SCH. In [7], Kai *et al.* proposed another analytical framework for efficient channel allocation across coexisting wideband WLANs to improve the overall performance. The work in [8] analyzes the performance of SCA for the unsaturated traffic condition.

In [10], Yang *et al.* showed that an enhanced RTS/CTS of 802.11ac cannot solve the performance degradation caused by hidden interference on SCHs when the receiver cannot sense that hidden interference. They proposed to adaptively decrease the channel width when the hidden interference on an SCH is detected, and turn on/off the RTS/CTS based on the inferred knowledge about the presence/absence of hidden interference on a PCH. The performance degradation caused by a time-domain interference, which does not overlap with the desired signal in the frequency domain, was studied in [11]. To overcome such the adverse impact of time-domain interference, the authors proposed an algorithm for adapting the operating channel bandwidth.

In [16] and [17], the authors experimentally showed that transmitting over a 40MHz channel of 802.11n results in the degraded received signal quality compared to the transmissions over a 20MHz channel; consequently, the transmission coverage shrinks and the packet loss increases. They also showed that DCA could achieve significant throughput gains if a transmitter properly adjusts its transmission power and data rate while sending over a 40MHz-wide channel.

All of the above-mentioned works in literature aim to solve different important problems of wideband WLANs. However, the fundamental problem related to the vulnerability of the wideband PHY packet structure to narrowband interference/collision, which was discussed in Section II-D, is not yet touched in the related literature. To mitigate the severe impact of narrowband interference on wideband transmission, we propose a parallel PPDU transmission scheme which is explained in detail in the following section.

III. PARALLEL PPDU TRANSMISSION FOR WIDEBAND WLANS

A. PROPOSED SCHEME

The previous section discussed the baseline wideband PPDU transmission scheme and its vulnerability to a collision/interference in any of the subchannels. To mitigate such the vulnerability problem of wideband PPDUs, we propose a new parallel PPDU transmission scheme. Unlike the baseline 40, 80, or 160MHz-wide PPDU transmissions, the proposed parallel PPDU transmission scheme transmits several 20MHz PPDUs in a parallel manner, where each of the parallel PPDUs carries a separate A-MPDU. Every PPDU takes the 20MHz VHT format, thus there will be no additional overhead in terms of PHY preambles. An example of the PHY packet structure of 80MHz parallel PPDU transmission is shown in Figure 5. The length of VHT DATA and the contents of legacy and VHT preambles are the same for all PPDUs. How the sender achieves the same-sized VHT DATAs across all PPDUs will be discussed in the following paragraphs.

1) THE SENDER AND RECEIVER OPERATIONS

The sender uses the same medium access protocol (i.e., CSMA/CA-based DCF) and the same wideband channel access mechanisms such as SCA and DCA. The parallel PPDU formation is done as follows. The sender calculates the number of MPDUs to be aggregated in each PPDU. Then, the sender composes a VHT A-MPDU for each subchannel starting from the PCH. When composing A-MPDUs, the oldest MPDUs are aggregated first. The number of parallel PPDUs simply equals the number of 20MHz channels that

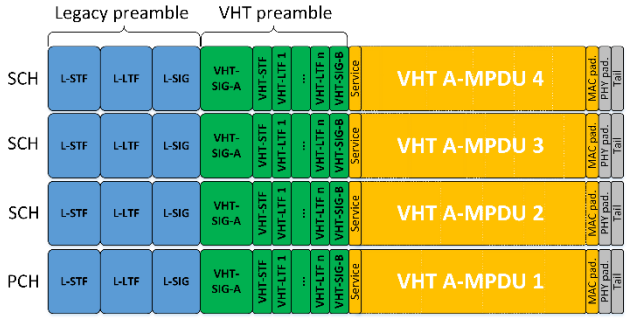

FIGURE 5. PHY packet structure of 80MHz parallel PPDU transmission.

will be used. However, sometimes, all usable channels will not be utilized. Consider a case, when the number of available MPDUs is smaller than the number of 20MHz channels that are available for transmission; in such a case, the number of usable SCHs is decreased to form the next narrower valid bandwidth. For example, if the sender has three MPDUs and four available 20MHz channels in total, it decreases the total bandwidth from 80MHz to the next narrower valid bandwidth, i.e., to 40MHz; the first two MPDUs will be aggregated into the A-MPDU of PCH and the remaining MPDU will be transmitted in the A-MPDU of the first SCH. Such an approach will enable us to continue utilizing the 2-bit BW subfield of VHT-SIG-A in the VHT preamble to specify one of the four valid bandwidths: 20, 40, 80, and 160MHz.

Similar to the existing scheme, if the receiver correctly receives at least one MPDU, it replies with a 20MHz BlockACK frame replicated over each of the subchannels that are utilized during transmission of the sender. The receiver learns about the total bandwidth from the BW subfield of one of the successfully decoded VHT preambles. When successfully receiving any of the BlockACK frames, the sender can identify how many MPDUs of each A-MPDU were successful. If no MPDU of PCH A-MPDU was successful or no BlockACK was received within the timeout, the sender increases the backoff stage. In all other cases, the sender resets its backoff stage.

It is noted that MIMO can be applied to baseline wideband 802.11n/ac transmissions to achieve higher throughput. As well known, the MIMO is a technology for multiplexing several data streams using multiple pairs of transmit and receive antennas. Since the proposed scheme can be applied to each of the multiple data streams separately which then can be multiplexed by MIMO, the MIMO is applicable to the proposed scheme too.

2) OVERHEAD IN THE PROPOSED SCHEME

One of the limitations of the proposed scheme is the overall decreased VHT PPDU payload transmission rate. In the proposed scheme, all PPDUs are transmitted in the standard 20MHz VHT format. In the 20MHz VHT format, a total of 56 orthogonal frequency division multiplexing (OFDM) subcarriers are utilized: 52 of them are used to carry data bits, while the other four are used as the pilots for phase rotation, frequency offset, and symbol timing correction throughout the PPDU reception [12]. As Table 1 shows, in the baseline 802.11ac, as the bandwidth increases from 20 to 40MHz, the number of data subcarriers increases from 52 to 108, but the number of pilot subcarriers increases from four to six only. On the other hand, in the proposed scheme, the numbers of data and pilot subcarriers are respectively doubled resulting in fewer data subcarriers; this leads to about a 3.70% decrease in an overall VHT PPDU payload transmission rate. For both 80 and 160MHz bandwidths, the decrease is about 11.11%. However, thanks to more pilot subcarriers, the proposed parallel PPDU transmission is more reliable than the baseline wideband transmission.

TABLE 1. Data and pilot subcarrier comparison.

BW (MHz)	Baseline 802.11ac		Proposed scheme		PHY rate decrease (%)
	Data	Pilot	Data	Pilot	
20	52	4	52	4	0.00%
40	108	6	104	8	3.70%
80	234	8	208	16	11.11%
160	468	16	416	32	11.11%

Another overhead is related to paddings. When A-MPDUs in parallel PPDUs have different sizes, the paddings are appended to make the PPDUs of the same size. Instead of adding the paddings that do not carry useful information, it is also possible to append a copy of one of the MPDUs and thus make its successful delivery more possible; but we do not consider such a scheme in this work.

B. THROUGHPUT ANALYSIS OF WIDEBAND 802.11ac AND 802.11a WLANs COEXISTING ON THE PCH

1) SYSTEM MODEL

We consider two WLANs of different technologies, namely IEEE 802.11a and 802.11ac WLANs coexisting together. The legacy (IEEE 802.11a) stations operate on the PCH of IEEE 802.11ac (shortly, 11ac) stations. The number of legacy stations and the number of 11ac stations are denoted by n_{leg} and n_{ac}, respectively. We make the following assumptions:

1. All stations are within range of each other.
2. Channel quality is ideal and therefore, packet loss happens only due to a collision.
3. Stations have saturated buffers; thus, they always contend for channel access.

Upon the channel access, a legacy station transmits a single MPDU and an 11ac station transmits 64 MPDUs. In the case of the proposed scheme, an 11ac station transmits two A-MPDUs each with 32 MPDUs if a 40MHz channel is

used, or four A-MPDUs each with 16 MPDUs if an 80MHz channel is used.

2) THROUGHPUT ANALYSIS MODEL FOR THE BASELINE SCHEME

Since the legacy stations operate on the PCH of 11ac WLAN, the legacy and 11ac stations share the PCH using the same DCF channel access mechanism. Thus, we can use the Bianchi's Markov chain model in [18] as a basis for analyzing the throughput performance of our system. According to [18], each station has the following transmission probability in any given time slot

$$\tau = \frac{2(1-2p)}{(1-2p)(W+1)+pW(1-(2p)^m)}, \tag{1}$$

where p, W, and m represent the probability that the transmitted frame suffers from a collision, the minimum contention window size, and the maximum backoff stage, respectively. The conditional probability that the transmitted frame encounters collision is given by

$$p = 1-(1-\tau)^{n-1}, \tag{2}$$

where n represents the number of all stations, i.e., $n = n_{leg} + n_{ac}$. The probability that at least one of the stations transmits in the given slot is

$$P_{tr} = 1-(1-\tau)^n. \tag{3}$$

Three types of slots are differentiated:

1. An idle slot is observed when none of the stations transmits, i.e., all n stations are counting down their backoff slots:

$$P_I = 1-P_{tr} = (1-\tau)^n. \tag{4}$$

   The corresponding idle slot duration simply equals the standard slot duration: $T_I = \sigma$.

2. A success slot is observed if only one station transmits:

$$P_S = \binom{n}{1}\tau^1(1-\tau)^{n-1} = n\tau(1-\tau)^{n-1}. \tag{5}$$

   The success slot may have one of two durations depending on whether the transmitting station is a legacy or 11ac. Since each station has an equal chance for transmission, the expected duration of success slot is given as follows.

$$T_s = \frac{n_{leg}T_{leg}}{n} + \frac{n_{ac}T_{ac}}{n} + DIFS, \tag{6}$$

   where T_{leg} and T_{ac} are the sum of the PPDU, the SIFS, and the ACK/BlockACK frame durations for a legacy station and an 11ac station, respectively.

3. A collision slot is observed when two or more stations transmit simultaneously. Alternatively, if idle and success slots are not observed, the collision slot is observed:

$$P_C = 1-P_I-P_S = P_{tr}-P_S. \tag{7}$$

Similarly to the case of success slot, the collision slot can also have one of two possible durations, depending on the types of stations in a collision. Note that the collision duration (T_{coll}) is equal to the longest duration of the transmissions involved in the collision. The following equations (8) and (9) express the probability distributions of different collision durations

$$\begin{cases} \Pr\{T_{coll}=T_{leg}\} \\ =\Pr\{\textit{only legacy stations collide}\} \\ =\sum_{k=2}^{n_{leg}} P_k \frac{n_{leg}}{n}\frac{n_{leg}-1}{n-1}..\frac{n_{leg}-k+1}{n-k+1} \\ =\sum_{k=2}^{n_{leg}} P_k \frac{n_{leg}!}{n!}\frac{(n-k)!}{(n_{leg}-k)!}, \\ \Pr\{T_{coll}=T_{ac}\}=1-\Pr\{T_{coll}=T_{leg}\} \end{cases} , T_{leg} < T_{ac} \tag{8}$$

$$\begin{cases} \Pr\{T_{coll}=T_{ac}\}=\sum_{k=2}^{n_{ac}} P_k \frac{n_{ac}!}{n!}\frac{(n-k)!}{(n_{ac}-k)!} \\ \Pr\{T_{coll}=T_{leg}\}=1-\Pr\{T_{coll}=T_{ac}\} \end{cases} , T_{leg} \geq T_{ac} \tag{9}$$

where P_k is the probability that exactly k stations transmit simultaneously. That is,

$$\begin{aligned} P_k &= \Pr\{\text{exactly } k \text{ stations collide}\} \\ &= \frac{\binom{n}{k}\tau^k(1-\tau)^{n-k}}{P_C}. \end{aligned} \tag{10}$$

Finally, the expected duration of the collision slot is given by

$$\begin{aligned} T_C &= E[T_{coll}] \\ &= \Pr\{T_{coll}=T_{leg}\}T_{leg} + \Pr\{T_{coll}=T_{ac}\}T_{ac}. \end{aligned} \tag{11}$$

Since the total throughput of the system is the length of data payload (bits) successfully transmitted during a slot time,

$$S = \frac{E[\Lambda_{data}]}{E[T_{slot}]} = \frac{P_S\left[\frac{1}{n}\left(n_{leg}\Lambda_{leg}+n_{ac}\Lambda_{ac}\right)\right]}{P_I T_I + P_S T_S + P_C T_C}. \tag{12}$$

$E[\Lambda_{data}]$ represents the average size of the successfully transmitted MAC payload during $E[T_{slot}]$ which represents the average system slot duration. Λ_{leg} represents the size of the MAC payload in a PPDU of a legacy station and Λ_{ac} is the size of the total MAC payload within a PPDU of an 11ac station.

3) THROUGHPUT ANALYSIS MODEL FOR THE PROPOSED PARALLEL-PPDU TRANSMISSION SCHEME

The throughput analysis model of the proposed parallel-PPDU transmission scheme has a few major differences from the existing model given in the previous subsection. First, the collision and success slot durations are longer than those in the baseline scheme; that is because of the longer transmission duration T_{ac} caused by the slower overall PPDU

payload transmission rate and the larger PHY overhead, as was explained in Section III-A.

Second, the expected length of MAC payload successfully delivered over a slot time is longer than that in the baseline scheme. In the baseline scheme, a narrowband collision on PCH corrupts the whole wideband PPDU. Whereas, in the proposed scheme, such collision corrupts only the PPDU that is transmitted on PCH and the receiver can successfully decode all remaining PPDUs transmitted on SCHs. Thus, the expected payload length is given by

$$E\left[\Lambda_{data}\right] = P_S\left[\frac{1}{n}\left(n_{leg}\Lambda_{leg} + n_{ac}\Lambda_{ac}\right)\right] + \left(n_{ac}\tau\left(1-\tau\right)^{n_{ac}-1}\right) \cdot \left(1-\left(1-\tau\right)^{n_{leg}}\right) \cdot \frac{\left(n_{ch}-1\right)\Lambda_{ac}}{n_{ch}}. \quad (13)$$

The first component of summation in (13) represents the expected successful data payload length transmitted during the successful slot time. The second component represents the expected successful data payload length transmitted during the collision slot where the wideband parallel transmission collides with one or more 20MHz legacy transmissions. More specifically, $n_{ac}\tau\left(1-\tau\right)^{n_{ac}-1}$ represents the probability that only one of the n_{ac} stations transmits in a given slot, $\left(1-\left(1-\tau\right)^{n_{leg}}\right)$ represents the probability that at least one of the legacy stations also transmits causing a collision on the PCH, and $\left(1-\left(1-\tau\right)^{n_{leg}}\right)\left(n_{ch}-1\right)\Lambda_{ac}/n_{ch}$ represents the successful data payload length in such a collision, where n_{ch} is the number of subchannels occupied by the wideband transmission. All the symbols used in the model are summarized in Table 2.

TABLE 2. Notations used in system model.

Symbol	Description
DIFS	DIFS duration (34μs)
PIFS	PIFS duration (25μs)
SIFS	SIFS duration (16μs)
m	Maximum backoff stage (6)
n	Number of all stations
n_{ac}	Number of 11ac stations
n_{ch}	Number of 20MHz subchannels occupied by the wideband transmission
n_{leg}	Number of legacy stations
p	Conditional collision probability [18]
P_C	Collision slot probability
P_I	Idle slot probability
P_S	Success slot probability
P_{tr}	Probability of at least one transmission in slot
T_{ac}	Sum of the DATA PPDU, the SIFS, and the BlockACK frame durations for an 11ac station (s)
T_C	Collision slot duration (s)
T_{coll}	Collision duration which is determined by the longest transmission duration involved in a collision (s)
T_I	Idle slot duration (s)
T_{leg}	Sum of the DATA PPDU, the SIFS, and the ACK frame transmission duration for a legacy station (s)
T_{slot}	Generic slot duration (s)
T_S	Success slot duration (s)
W	Minimum contention window size (16)
σ	Empty backoff slot duration in standard (9μs)
Λ_{ac}	Length of MAC payload included in PPDU of 11ac station (bits)
Λ_{data}	Length of MAC payload included in generic PPDU
Λ_{leg}	Length of MAC payload included in PPDU of legacy station (800 bits)
τ	Transmission probability by a station [18]

IV. PERFORMANCE EVALUATIONS

A. SATURATED THROUGHPUT MODEL VALIDATION

In this subsection, we compare the analysis results from the model given in the previous section with the simulation results. For that purpose, we developed a discrete-event simulator written in Python programming language. Some simulation and model parameters are given in the System model of Section III-B and others are as follows:

- The legacy stations use the PHY transmission rate of 54Mbps.
- The 11ac stations transmit using 2 × 2 MIMO, MCS 7 (64 QAM modulation and 5/6 coding rate), and short GI, which result in the PHY transmission rate of 144.4Mbps for a 20MHz channel. In the baseline scheme, those transmission settings give the PHY transmission rates of 300 and 650Mbps for 40 and 80MHz channels, respectively. In the proposed scheme, since each of the parallel PPDUs is transmitted on the 20MHz channel at a 144.4Mbps PHY rate, the overall PHY transmission rate becomes 288.8Mbps (2 × 144.4) and 577.6Mbps (4 × 144.4) for total channel bandwidths of 40 and 80MHz, respectively.
- The queue size limits are 50 and 400 packets for legacy and 11ac stations, respectively.
- Each MPDU has 272 bits of MAC header and 8000 bits of payload.
- All simulations are run for three different seed values and 10 seconds duration.

As Figure 6 shows, the analysis results are closely matched to the simulation results. When there is no legacy station, the baseline 11ac provides better throughput performance, since the baseline 11ac transmits the PPDU payload at a higher PHY transmission rate, as discussed in the previous section. As the number of legacy stations starts increasing, the throughput gain of the baseline 11ac disappears and the

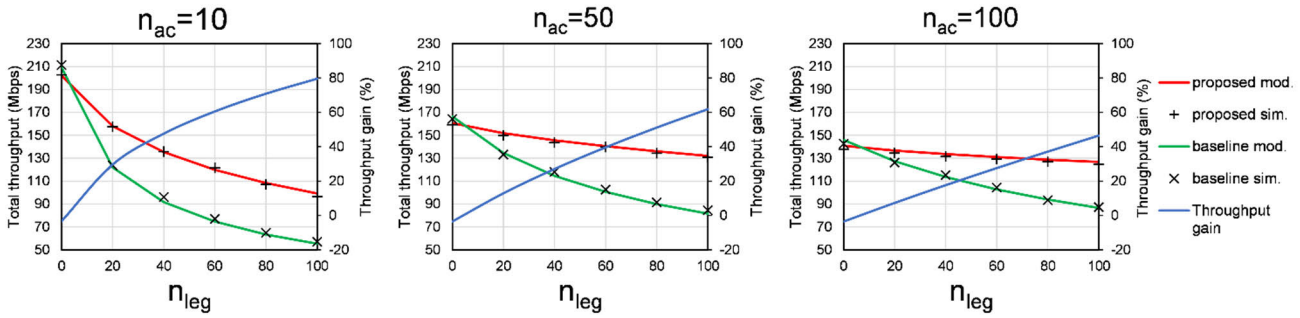

a) 11ac stations with 40MHz total bandwidth.

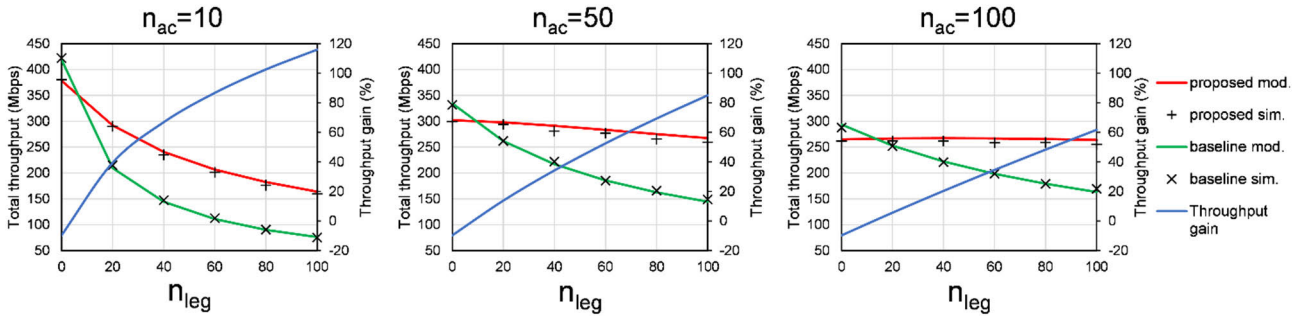

b) 11ac stations with 80MHz total bandwidth.

FIGURE 6. Total network throughput comparison of the simulation and analytical model for 'baseline' 11ac and the 'proposed' scheme.

proposed scheme starts achieving a significant throughput gain. That is because wideband transmissions start colliding with 20MHz legacy transmissions on the PCH; in the baseline 11ac, such collisions affect the whole wideband PPDU transmission, whereas, in the proposed scheme, they affect only the PCH PPDUs while the SCH PPDUs are successfully delivered.

The wider total channel bandwidth leads to more benefits from the proposed scheme. The throughput gain for 80MHz bandwidth depicted in Figure 6b is significantly bigger than that for the 40MHz case depicted in Figure 6a. For example, for $n_{leg} = 100$, the proposed scheme with 40MHz bandwidth has about 80, 62, and 46% improvement in the throughput performance over the baseline scheme for $n_{ac} = 10$, 50, and 100, respectively; in the 80MHz case, it has about 116, 85, and 63% improvement for $n_{ac} = 10$, 50, and 100, respectively.

B. PERFORMANCE EVALUATION FOR DIFFERENT TRAFFIC LOADS

In this subsection, we evaluate the performance of different traffic conditions through simulations only. The total offered traffic load of 11ac WLAN, $Load_{ac}$, is set to different loads such that 50, 100, and 300Mbps. The total offered traffic load of legacy WLAN, $Load_{leg}$, is set to one of 10, 15, and 20Mbps loads. Let us denote the size of the MPDU payload by Λ_{MPDU} (bits), then packet inter-arrival time is exponentially distributed with a mean of $\Lambda_{MPDU}/(Load_{ac}/n_{ac})$ and $\Lambda_{MPDU}/(Load_{leg}/n_{leg})$ at each of the 11ac and legacy stations, respectively. The other parameters are the same as in Section IV-A.

1) THROUGHPUT ANALYSIS

Figure 7 depicts the normalized throughput of an 802.11ac WLAN for different traffic loads ($Load_{ac} = 50$, 100, and 300Mbps) while varying the number of stations ($n_{ac} = 10, 50,$ and 100). Besides that, there are different numbers of legacy stations ($n_{leg} = 10, 50,$ and 100) contending for the PCH with a varying offered load ($Load_{leg} = 10$, 15, and 20Mbps). The 11ac stations have a total channel bandwidth of 80MHz.

When n_{leg} is larger than n_{ac}, the proposed scheme achieves much bigger throughput gains. Look at the first column charts of Figure 7a to Figure 7c, where $n_{ac} = 10$ and n_{leg} changes from 0 to 100. The higher the n_{leg} and $Load_{leg}$ are, the bigger the throughput improvement of the proposed scheme over the baseline scheme is. For example, when n_{leg} reaches 100 for $Load_{leg} = 20$Mbps, the throughput gain reaches 26, 56, and 90% for $Load_{ac} = 50$, 100, and 300Mbps, respectively. That can be explained as follows. When $n_{ac} < n_{leg}$, most of the airtime on PCH is dominated by legacy transmissions leaving less chance for the 11ac transmissions. Besides that, in the baseline scheme, the collision of a wideband PPDU with a 20MHz PPDU results in retransmission of both of the PPDUs, thus hampering the efficient resource utilization. Whereas,

Ratio of the 11ac network throughput to $Load_{ac}$

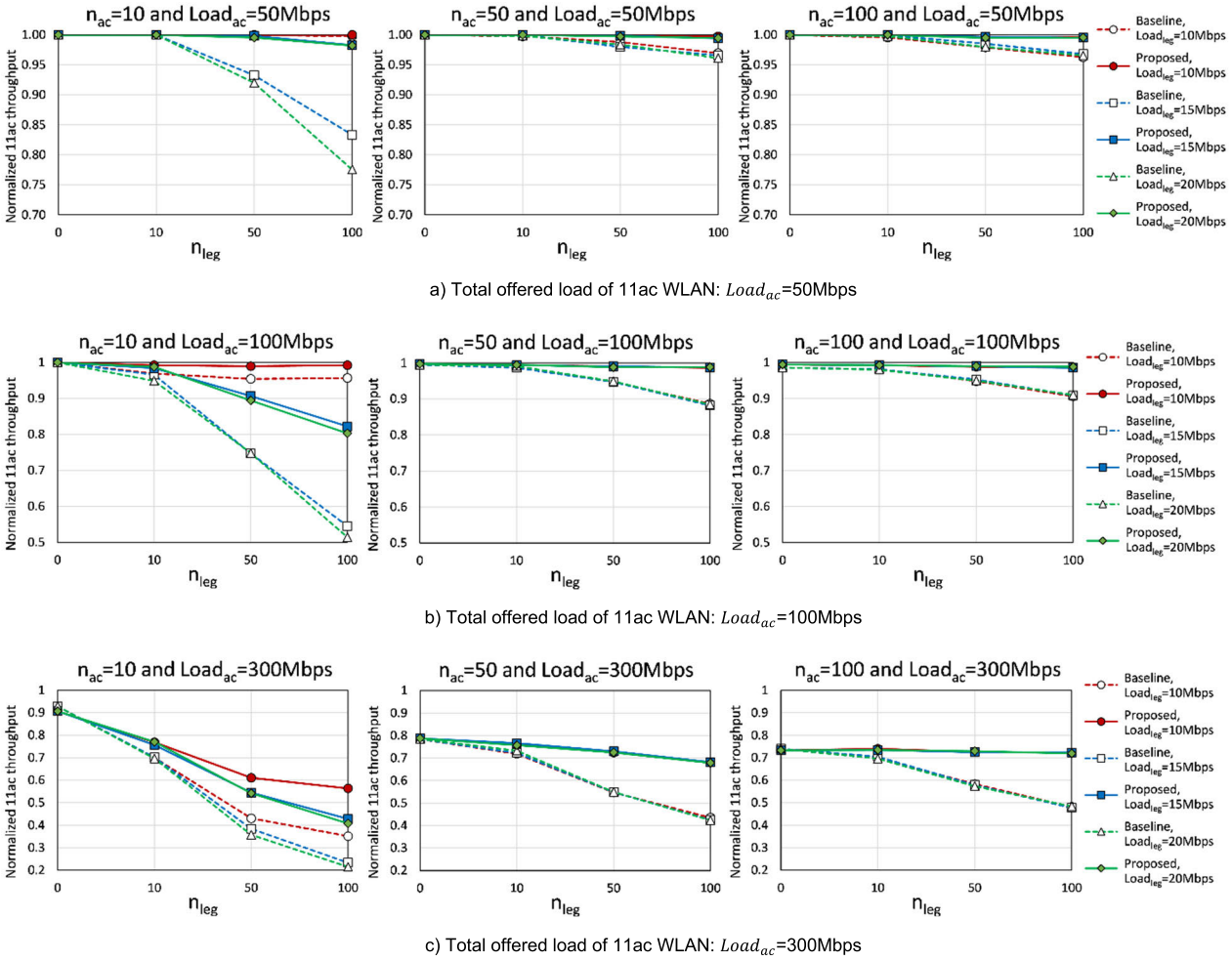

FIGURE 7. Normalized 802.11ac network throughput.

in the proposed scheme, if such a collision happens, only one parallel PPDU is corrupted, and thus, the packets of only the corrupted parallel PPDU and legacy PPDU are retransmitted. Since the packets of the corrupted parallel PPDU are re-distributed into parallel PPDUs again, their transmission durations are less than the corrupted parallel PPDU, and therefore the medium is utilized more efficiently.

As n_{ac} increases, the proposed scheme continues to achieve a significant throughput gain, especially much more for higher $Load_{ac}$. More precisely, when $Load_{ac}$ increases from 100 to 300Mbps, the throughput gain at $n_{ac} = 50$ increases from 10 to 60% while the throughput gain at $n_{ac} = 100$ increases from 8.5 to 50%. Most importantly, there is the following tendency for big n_{ac} values such as 50 and 100: as n_{leg} increases, the throughput of the baseline scheme decreases in a much faster fashion compared to the proposed scheme, which means the throughput gain of the proposed scheme continuously increases. Look at the case where $n_{ac} = 100$ and $Load_{ac} = 300$Mbps: as n_{leg} increases from 0 to 100, the throughput of the proposed scheme merely decreases by 1.3% while the baseline scheme decreases by 36%.

2) DELAY ANALYSIS

Figure 8 depicts the end-to-end packet transmission delay of 80MHz 11ac stations for $n_{ac} = 50$ and $Load_{ac} = 100$Mbps. n_{leg} is set to 50 and 100 while $Load_{leg}$ can be 10, 15, and 20Mbps. In the baseline scheme, when a wideband PPDU collides with legacy 20MHz transmissions, the whole wideband PPDU is corrupted and therefore retransmitted. Such a collision consequently increases the end-to-end delay of every packet (MPDU) included in that wideband PPDU. In contrast, in the proposed scheme, if wideband transmission collides with 20MHz transmission, only one PPDU is corrupted while the remaining parallel PPDUs are successfully delivered improving the delay performance of packets transmitted in those PPDUs. For example, when $n_{leg} = 50$, only about 77% of packets delivered under the baseline scheme have the end-to-end delay shorter than 0.5s, while the proposed scheme delivers about 97% of packets within such delay boundary, as depicted in Figure 8.

The increase in n_{leg} to 100 incurs more collisions with the wideband 11ac PPDUs and thus further deteriorates the delay performance of the baseline scheme. More precisely, the amount of packets with a delay shorter than 0.5s decreases

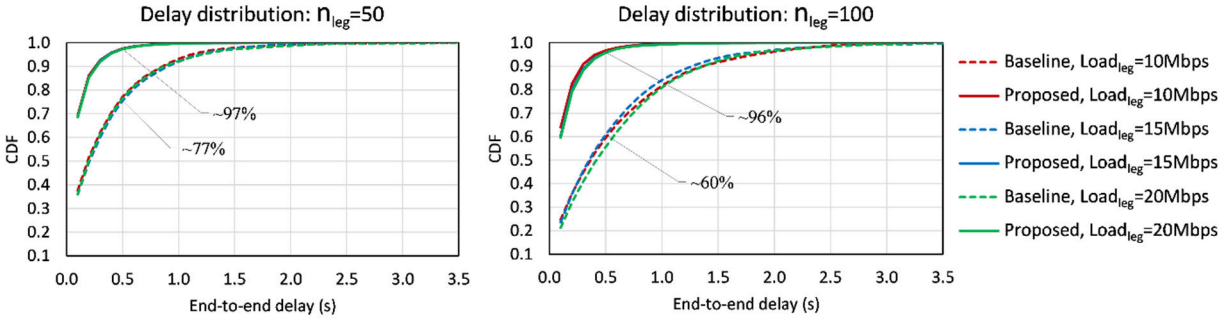

FIGURE 8. CDF of end-to-end packet delay of 80MHz 11ac traffic: $n_{ac} = 50$, $Load_{ac} = 100$Mbps.

from 77 to 60%; whereas in the proposed scheme, the amount of such packets merely decreases by about one percent.

3) AGGREGATION SIZE ANALYSIS

Figure 9 depicts the distribution of aggregation size. Note that in the baseline 802.11ac, the maximum aggregation size of a VHT A-MPDU is limited to 64. However, in the proposed scheme, the maximum aggregation size of each of the parallel VHT A-MPDUs varies depending on the total channel width. Each parallel VHT A-MPDU can have up to 8, 16, 32, and 64 packets for the total bandwidth of 160, 80, 40, and 20MHz, respectively. Therefore, the aggregation size in this context represents the number of packets per transmission, which cannot exceed 64 in both schemes.

In the baseline scheme, when a wideband PPDU collides with a narrowband transmission, a whole wideband PPDU is retransmitted upon the next channel access, including new packet(s) if there is any. When finally this wideband PPDU succeeds, its size is usually greater or equal to its initial size but not smaller. In contrast, in the proposed scheme, when a wideband transmission collides with a narrowband transmission, some of the parallel PPDUs are successfully delivered. Only the packets in unsuccessful PPDUs are retransmitted upon the next channel access together with new packets. Accordingly, after such a collision, the next transmission usually has a smaller aggregation size than the previous one. Therefore, the average aggregation size per transmission is significantly smaller than in the baseline scheme. More precisely, when $n_{leg} = 50$, the average aggregation size is about 17 and 7 in the baseline and the proposed schemes, respectively. When congestion on PCH increases further, both of the schemes tend to contain more packets per transmission. Thus, when n_{leg} increases to 100, the baseline 11ac station transmits 27.8 packets per transmission, whereas a station with the proposed scheme transmits only 10.5 packets on average.

C. PERFORMANCE EVALUATIONS OF MULTI-BSS SCENARIO WITH HIDDEN INTERFERENCE

1) ADDITIONS TO SIMULATOR

In the performance evaluations discussed in the previous subsections, we considered a single basic service set (BSS) where all stations perfectly sense each other. However, such an assumption is not usually applied to real-world applications of 802.11 deployments. Generally, multiple BSSs coexist together using the same or overlapping channels, the stations are scattered and it may be impossible that they cannot hear the transmission of each other, thus creating an undesirable interference at a receiver on both PCH and SCHs. To evaluate the performance of the proposed scheme under such situations, we made several changes in our simulator. Based on the standard [2] and default configurations of the *wifi* module in the ns-3 simulator [19], we adopted the following major changes in our simulator:

- Additive white Gaussian noise (AWGN) channel model.
- Log-distance path loss model with path loss exponent of 3.0.
- CCA energy detection (ED) mechanism with the sum receive (RX) power threshold of −62dBm for both PCH and SCH [1], [12].
- CCA signal detection (SD) mechanism with 4μs window for PCH, where the RSS threshold is −82dBm and the signal-to-noise-plus-interference ratio (SNIR) threshold is 4dB. This results in different transmit ranges depending on total bandwidth, as shown in Table 3 [1], [12].
- CCA-SD mechanism with 25μs window for SCH, where the RSS threshold is −72dBm [2], [12].
- A more realistic OFDM error model [20] developed by the National Institute of Science and Technology (NIST) and adopted in ns-3 as the default error model [19], [21].

Using the conditions of CCA-SD, the receiver locks to the strongest signal which satisfies SNIR ≥ 4dB within the CCA window duration of 4μs. This is called signal/preamble detection. When no signal meets this requirement, the listening station does one of the followings: if the current sum RX power is less than the CCA-ED threshold, i.e., −62dBm, the station sets the medium idle and resumes its frozen backoff process; otherwise, the station stays busy while the CCA-ED condition is satisfied. Even after the listening station locks to transmission, it continues using CCA-SD during L-STF and L-LTF durations, to lock to a much stronger signal if there is any; in other words, if the station finds a signal with stronger RSS and SNIR ≥ 4dB, it abandons the ongoing

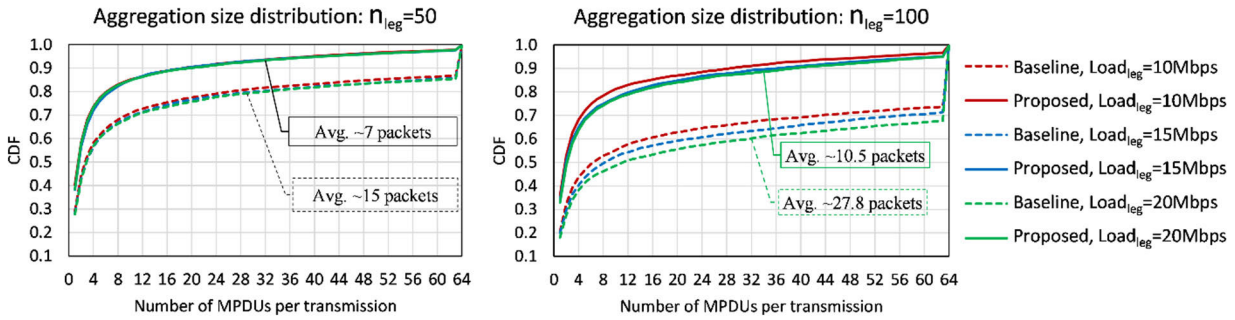

FIGURE 9. CDF of aggregation size of 80MHz 11ac transmissions: $n_{ac} = 50$, $Load_{ac} = 100$Mbps.

TABLE 3. Simulation settings.

Parameter	Value
Transmit power	40mW
Channel	AWGN channel
Propagation model	Log-distance path loss model with path loss exponent of 3.0, reference distance of 1.0m, and reference loss of 46.68dB
Rx sensitivity	-101.0dBm
CCA-ED	Sum RX power ≥ -62dBm
CCA-SD for PCH	RSS ≥ -82dBm and SNIR ≥ 4dB
CCA-SD for SCH	RSS ≥ -72dBm
CCA-ED range	11.1m, 8.8m, and 7.0m for 20, 40, and 80MHz transmissions, respectively
CCA-SD range on clean PCH	51.4m, 40.8m, and 32.4m for 20, 40, and 80MHz transmissions, respectively
CCA-SD range on clean SCH	23.9m, 19.0m, and 15.1m for 20, 40, and 80MHz transmissions, respectively
Noise figure	7dB
Error model	NIST error model [19], [20], [21]
$Load_{ac}$	Total offered load of 11ac stations in single BSS (20 and 50Mbps)
$Load_{leg}$	Total offered load of legacy stations in single BSS (5Mbps)
n_{ac}	Number of 11ac stations in single BSS (10 and 20)
n_{leg}	Number of legacy stations in single BSS (0, 10, 20,.., 50)

signal reception and locks to a new signal. This is called a frame capture.

After the reception of the legacy preamble ends, the station checks if the L-SIG field was successfully decoded. The L-SIG field is nothing but a small data field with 24 bits, which includes information about the duration of the remaining transmission. The reception status of a data field is decided as follows. As in ns-3, data duration in our simulation is divided into so-called chunks. A chunk is an interval during which the

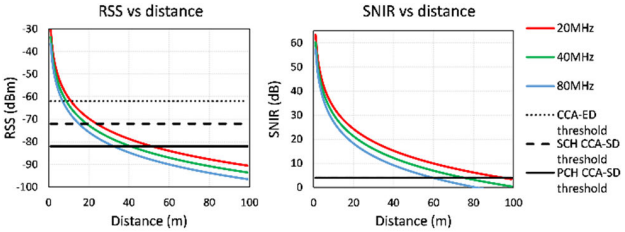

FIGURE 10. RSS and SNIR decay for different channel widths and distance.

SNIR of a locked signal stays unchanged. First, a bit error rate (BER) of each chunk is calculated by the NIST error model based on SNIR and MCS [19]–[21]. The chunk success rate (CSR) is calculated for each chunk, depending on the number of bits it has: $CSR_i = (1 - BER)^{bits_i}$. Finally, a success rate of the data field is obtained: $FSR = \prod_i^n CSR_i$. Then a random number, *rand*, is chosen within an interval of (0, 1] and the field is assumed to be successfully received if the *rand* > FSR, otherwise unsuccessful. If L-SIG is successful, the receiving station knows the remaining duration and the data rate, so it continues decoding the PPDU; otherwise, it ceases the reception and decides whether to stay idle or busy using the CCA-ED mechanism.

In the case of VHT PPDU, the legacy preamble is followed by the VHT preamble, which has VHT-SIG, VHT-STF, and VHT-LTF fields. The reception status of all those fields is decided using the NIST error model as it is done for L-SIG. If any of those fields is received with error, decoding of the remaining part of the PPDU fails. In the baseline scheme, the erroneous reception of any of the fields in the legacy or VHT preamble applies to the whole wideband PPDU, whereas in the proposed scheme, a decoding error for the preamble of one of the parallel PPDUs applies to the corresponding PPDU only. In the case of a successful preamble (legacy and VHT), the receiver continues decoding the data part of the PPDU. The success/failure status of each MPDU is also decided using the NIST error model. The above mentioned major changes and some others are summarized in Table 3.

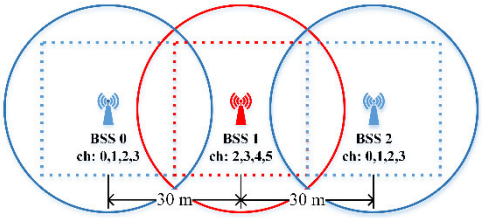

FIGURE 11. Multi-BSS topology with hidden nodes.

Figure 10 shows the RSS and SNIR decay of different channel width as the distance between the transmitter and the receiver increases. Note that the SNIR plot is drawn with an assumption of a clean channel, i.e., there is no interfering transmission. As shown in Table 3 and Figure 11, for a clean channel, owing to the PCH CCA-SD mechanism, the 20MHz signal can be detected at as far as about 51.4m distance, while the maximum detectable distance of 40 and 80MHz signals can be as long as 40.8 and 32.4m, respectively. This means if the channel width doubles, the detectability of the signal decreases by about 10m. The wideband station senses its SCH busy if there is a 20MHz transmission by a station located at most 23.9m far. To sense the PCH or SCH as busy using CCA-ED, a 20MHz transmission should occur from at most 11.1m distance such that the RSS will not be less than −62dBm. That is, the clean channel detection depends on the channel bandwidth and channel type (PCH or SCH) as well as the CCA thresholds.

2) SIMULATION TOPOLOGY AND PERFORMANCE EVALUATIONS

There are three cells of 30mx30m size as depicted in Figure 11. An AP is located at the center of each cell. The APs support the 802.11ac 80MHz capability and are compatible with legacy 802.11a devices. The BSS ID and operating channels of each BSS are specified. For instance, the BSS 0 operates on 20MHz channels 0, 1, 2, and 3, where channel 0 is configured as PCH and channels 1 to 3 are SCHs. Here, the channels n and $n+1$ represent two adjacent and orthogonal 20MHz-wide channels with 20MHz space between their central frequencies.

Each AP serves n_{ac} 11ac stations and n_{leg} legacy stations that are randomly placed in the corresponding cell area. $Load_{ac}$ represents the total offered load of all 11ac stations per BSS. For each ($Load_{ac}$, n_{ac}) pair, the BSS throughputs of the baseline and the proposed schemes are measured for different n_{leg} values. $Load_{leg}$ is the total offered load of all legacy stations per BSS and is fixed to 5Mbps. Each simulation is conducted for three different seed values and five seconds duration. Other parameters are the same as in Sections IV-A and IV-B.

Figure 12 depicts the normalized 11ac throughputs per BSS averaged for three seeds. Let us first discuss Figure 12a where $Load_{ac} = 20$Mbps. For the small number of 11ac stations (i.e., $n_{ac} = 10$) and no legacy stations (i.e., $n_{leg} = 0$), there are a few collisions and low interference. Furthermore, because a very high PHY transmission rate is used, all three BSSs can serve almost all of the offered traffic load. However, as n_{leg} increases, the number of transmissions quickly increases in all BSSs, resulting in more collisions/interferences. The BSS 0 and BSS 1 under the baseline scheme suffer from more severe performance degradation. This is explained as follows. As compared with wideband stations, the legacy stations use the same tx power but much narrower channel (i.e., 20MHz-wide channel), and thus their transmissions propagate much farther increasing interference and blocking more stations from transmitting. Since BSS 0 and BSS 2 use the same channels, the legacy stations of those two BSSs can even block the stations of another cell from transmitting by triggering CCA-SD. If the wideband transmission collides with the legacy transmission of the same BSS, the wideband transmission will likely fail since there is a big chance the receiver will lock to a legacy transmission which has usually higher RSS than 11ac transmission due to its much smaller bandwidth. In contrast, if the wideband transmission collides on PCH with a legacy transmission from another BSS, then the baseline scheme will probably fail due to the preamble decoding error whereas the unaffected PPDUs of the proposed scheme will likely succeed.

Besides the impact of BSS 0 and BSS 2 on the performance of each other, BSS 1 also adversely affects the performance of both BSS 0 and BSS 2. As n_{leg} increases in BSS 1, more wideband stations of BSS 0 and BSS 2 near the boundary of BSS 1 have less chance to use a full 80MHz bandwidth since they will mostly sense the channel 2 as busy. If the interference by BSS 1 on channels 2 and 3 is less than −72dBm, the 11ac stations of BSS 0 and BSS 2 can utilize

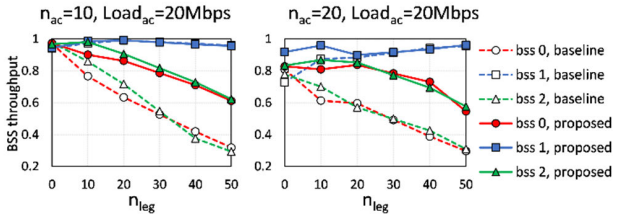

a) Total 11ac offered load per BSS: $Load_{ac}$=20Mbps and total legacy offered load per BSS: $Load_{leg}$=5Mbps

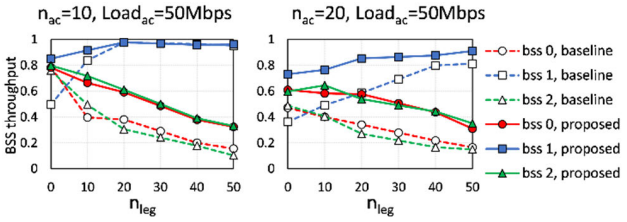

b) Total 11ac offered load per BSS: $Load_{ac}$=50Mbps and total legacy offered load per BSS: $Load_{leg}$=5Mbps

FIGURE 12. Normalized 11ac throughput per BSS.

a full bandwidth of 80MHz, however, it is more likely that the receiving wideband stations cannot correctly decode the preamble due to that interference. In the baseline scheme, such a case most probably causes the failure of full 80MHz PPDU, whereas, in the proposed scheme, the PPDUs on channels 2 and 3 are merely affected.

When $Load_{ac} = 50$Mbps in Figure 12b, a similar performance trend can be observed. However, the performance of BSS 1 under the baseline scheme is much smaller for small n_{leg} values. The reason is as follows. Due to a high $Load_{ac}$ per BSS and the increased interference caused by BSSs 0 and 2 on channels 2 and 3, a significant portion of the wideband transmissions in BSS 1 fail under the baseline scheme, while under the proposed scheme, the PPDUs on channels 4 and 5 will likely succeed. As n_{leg} increases, most of the airtime in BSSs 0 and 2 will be dominated by legacy transmissions while leaving less airtime for wideband transmissions, which results in decreased interference for wideband transmissions of BSS 1 and thus increasing its 11ac throughput.

V. CONCLUSION

In this article, we have addressed the vulnerability of 802.11n/ac wideband transmission to a narrowband collision. According to the current IEEE 802.11n/ac standard, when a wideband PPDU transmission on multiple narrowband channels encounters a collision on one of the narrowband channels, the whole wideband PPDU is affected. To mitigate such vulnerability of wideband transmissions, we proposed a parallel PPDU transmission scheme, which transmits multiple 20MHz PPDUs in parallel instead of a single wideband PPDU. As a result, collision on subchannels affects 20MHz PPDUs that are transmitted on those subchannels while other 20MHz PPDUs can be successfully delivered.

We analytically derived the throughput performance of the proposed scheme when wideband transmissions are intermixed with narrowband transmissions under the saturated load condition. We also evaluated the performance under various unsaturated traffic loads, by using simulation. The simulation results demonstrated that the proposed scheme improves remarkably not only the throughput performance but also the end-to-end delay performance, compared with the baseline wideband scheme. Additionally, evaluations in the more realistic multi-BSS environment have shown that the proposed scheme achieves significant throughput improvement in the presence of channel errors and hidden nodes too.

A prototype implementation of the proposed scheme can be effective in proving the concept of the scheme by demonstrating its real performance. We will consider implementing the proposed scheme with software-defined radio as our future work.

REFERENCES

[1] *Enhancement for Higher Throughput*, IEEE Standard Amendment 802.11n, Oct. 2009.
[2] *Enhancements for Very High Throughput Operation in Bands Below 6 GHz*, IEEE Standard Amendment 802.11ac, Dec. 2013.
[3] S. Barrachina-Munoz, F. Wilhelmi, and B. Bellalta, "Dynamic channel bonding in spatially distributed high-density WLANs," *IEEE Trans. Mobile Comput.*, vol. 19, no. 4, pp. 821–835, Apr. 2020.
[4] A. Faridi, B. Bellalta, and A. Checco, "Analysis of dynamic channel bonding in dense networks of WLANs," *IEEE Trans. Mobile Comput.*, vol. 16, no. 8, pp. 2118–2131, Aug. 2017.
[5] S. Pollin and A. Bahai, "Performance analysis of double-channel 802.11n contending with single-channel 802.11," in *Proc. IEEE Int. Conf. Commun.*, Dresden, Germany, Jun. 2009, pp. 1–6.
[6] M. Han, S. Khairy, L. X. Cai, and Y. Cheng, "Performance analysis of opportunistic channel bonding in multi-channel WLANs," in *Proc. IEEE Global Commun. Conf. (GLOBECOM)*, Washington, DC, USA, Dec. 2016, pp. 1–6.
[7] C. Kai, Y. Liang, X. Hu, Z. Liu, and L. Wang, "An effective channel allocation algorithm to maximize system utility in heterogeneous DCB WLANs," *Comput. Netw.*, vol. 153, pp. 23–35, Apr. 2019.
[8] M.-S. Kim, T. Ropitault, S. Lee, and N. Golmie, "A throughput study for channel bonding in IEEE 802.11ac networks," *IEEE Commun. Lett.*, vol. 21, no. 12, pp. 2682–2685, Dec. 2017.
[9] M. X. Gong, B. Hart, L. Xia, and R. Want, "Channel bounding and MAC protection mechanisms for 802.11ac," in *Proc. IEEE Global Telecommun. Conf.*, Dec. 2011, pp. 1–5.
[10] C. Yang, S. Kim, S. Byeon, and S. Choi, "HIATus: Hidden interference-aware transmission bandwidth adjustment in IEEE 802.11ac WLANs," *IEEE Commun. Lett.*, vol. 23, no. 3, pp. 510–513, Mar. 2019.
[11] S. Byeon, H. Kwon, Y. Son, C. Yang, and S. Choi, "RECONN: Receiver-driven operating channel width adaptation in IEEE 802.11ac WLANs," in *Proc. IEEE INFOCOM-IEEE Conf. Comput. Commun.*, Honolulu, HI, USA, Apr. 2018, pp. 1655–1663.
[12] E. Perahia and R. Stacey, *Next Generation Wireless LANs: 802.11n and 802.11ac*. Cambridge, U.K.: Cambridge Univ. Press, 2013.
[13] *Atheros Ath9K Driver*. Accessed: Aug. 2020. [Online]. Available: https://wireless.wiki.kernel.org/en/users/drivers/ath9k
[14] *iPerf—The Ultimate Speed Test Tool for TCP, UDP and SCTP*. Accessed: Aug. 2020. [Online]. Available: https://iperf.fr/
[15] S. Seytnazarov, J.-G. Choi, and Y.-T. Kim, "Enhanced mathematical modeling of aggregation-enabled WLANs with compressed BlockACK," *IEEE Trans. Mobile Comput.*, vol. 18, no. 6, pp. 1260–1273, Jun. 2019.
[16] M. Y. Arslan, K. Pelechrinis, I. Broustis, S. V. Krishnamurthy, S. Addepalli, and K. Papagiannaki, "Auto-configuration of 802.11n WLANs," in *Proc. 6th Int. Conf. Co-NEXT*, 2010, pp. 1–12.
[17] L. Deek, E. Garcia-Villegas, E. Belding, S.-J. Lee, and K. Almeroth, "The impact of channel bonding on 802.11n network management," in *Proc. 7th Conf. Emerg. Netw. Exp. Technol. (CoNEXT)*, 2011, pp. 1–12.
[18] G. Bianchi, "Performance analysis of the IEEE 802.11 distributed coordination function," *IEEE J. Sel. Areas Commun.*, vol. 18, no. 3, pp. 535–547, Mar. 2000.
[19] *Ns3—Network Simulator*. Accessed: Aug. 2020. [Online]. Available: http://www.nsnam.org
[20] L. E. Miller. (2003). *Validation of 802.11a/UWB Coexistence Simulation*. [Online]. Available: https://www.nist.gov/publications/validation-80211auwb-coexistence-simulation
[21] G. Pei and T. R. Henderson, "Validation of OFDM error rate model in ns-3," Boeing Res. Technol., Seattle, WA, USA, 2010. [Online]. Available: https://www.nsnam.org/~pei/80211ofdm.pdf

SHINNAZAR SEYTNAZAROV received the B.S. degree in communication engineering from the Tashkent University of Information Technologies, Uzbekistan, in 2010, and the M.S. and Ph.D. degrees in information and communication engineering from Yeungnam University, South Korea, in 2014 and 2018, respectively.

He is currently a Postdoctoral Research Fellow with the Department of Computer Science and Engineering, Seoul National University, South Korea. His research interests include resource management, performance modeling, and evaluation of random access MAC protocols in wireless and mobile networks.

DONG GEUN JEONG (Senior Member, IEEE) received the B.S., M.S., and Ph.D. degrees from Seoul National University, Seoul, South Korea, in 1983, 1985, and 1993, respectively.

From 1986 to 1990, he was a Researcher with the Research and Development Center of DACOM, South Korea. From 1994 to 1997, he was with the Research and Development Center, Shinsegi Telecomm Inc., South Korea, where he conducted and led research on advanced cellular mobile networks. In 1997, he joined the Hankuk University of Foreign Studies, South Korea, as a Faculty Member, where he is currently a Professor with the Department of Electronics Engineering. His research interests include resource management for wireless and mobile networks, the Internet of Things, and wireless technologies for industry.

Dr. Jeong has served on the Editorial Board for the *Journal of Communications and Networks* (JCN), from 2002 to 2007.

WHA SOOK JEON (Senior Member, IEEE) received the B.S., M.S., and Ph.D. degrees in computer engineering from Seoul National University, Seoul, South Korea, in 1983, 1985, and 1989, respectively.

From 1989 to 1999, she was with the Department of Computer Engineering, Hansung University, Seoul. In 1999, she joined Seoul National University, as a Faculty Member, where she is currently a Professor with the School of Electrical Engineering and Computer Science. Her research interests include resource management for wireless and mobile networks, high-speed networks, communication protocols, network performance evaluation, and the Internet of Things.

Dr. Jeon has served on the Editorial Board for the *Journal of Communications and Networks* (JCN), from 2002 to 2017.